Check for updates

Activatable supramolecular photosensitizers: advanced design strategies

Mengyao Yang,[a] Xingshu Li [iD] *[b] and Juyoung Yoon [iD] *[a]

Activatable photosensitizers (aPSs) are a new, switchable smart photosensitizer (PS) that can enhance photodynamic therapy (PDT) specificity and efficiency. aPSs are inert in healthy tissues, but can be switched on by neoplastic-associated endogenous stimuli such as pH, enzymes, and glutathione (GSH) and reduce damage to normal cells. This review summarizes aPS-based design strategies based on energy or electron transfer and self-quenching. We supplement the advanced design strategies with newly-developed molecular aPSs and focus on introducing nano-engineering supramolecular aPS construction.

1 Introduction

1.1 Photodynamic therapy (PDT) action mechanism

Cancer, one of the deadliest diseases, has attracted tremendous attention around the world. Photodynamic therapy (PDT) is a promising clinical treatment with non-invasive characteristics, spatiotemporal selectivity, minimal side effects, immunogenicity, negligible drug resistance and a rapid, scar-free healing process.[1–8] Modern PDT applications date back to the 1960s when Schwartz

and Lipson discovered a hematoporphyrin derivative (HPD).[9–11] Over the past 30 years, clinical treatments have used PDT on breast, prostate, bladder, and skin cancer tumors.[12–16]

The core PDT components are photosensitizers (PSs). PSs generate reactive oxygen species (ROS) when they are irradiated at particular light wavelengths. The PSs absorb photons, which excite their electrons and transform them from the ground state to an excited singlet state. Excited PSs are unstable and can return to their ground state using fluorescence emission or thermal decay to release energy.[17] Excited PSs can also undergo intersystem crossing (ISC) to reach a more stable excited triplet state. Excited PS triplets can generate phosphorescence or ROS.[18,19] ROS are generated *via* two processes and mechanisms, Type I and Type II.[20,21] The Type I mechanism refers to the excited triplet state reacting directly with the peripheral substance in a

[a] *Department of Chemistry and Nanoscience, Ewha Womans University, Seoul 03760, Republic of Korea. E-mail: jyoon@ewha.ac.kr*

[b] *College of Chemistry, State Key Laboratory of Photocatalysis on Energy and Environment, Fujian Provincial Key Laboratory of Cancer Metastasis Chemoprevention and Chemotherapy, Fuzhou University, Fuzhou 350108, China. E-mail: xingshuli@fzu.edu.cn*

Mengyao Yang received her MS degree of science in engineering from the Institute of Process Engineering (IPE), Chinese Academy of Sciences (CAS). She has been conducting her PhD research under the supervision of Prof. Juyoung Yoon at Ewha Womans University since 2019. She is now working on theranostics based on self-assembly of photosensitizer molecules.

Mengyao Yang

Xingshu Li is a Minjiang Distinguished Professor at Fuzhou University. He received his PhD degree from Fuzhou University in 2015. From 2016, he worked as a post-doctoral fellow at Ewha Womans University for 3 years, and then moved to University of Toronto in 2019. After completing post-doctoral research, Dr Li joined the College of Chemistry at Fuzhou University in 2020. His current interests include the design and development of innovative photosensitizers and theranostics based on functional dyes.
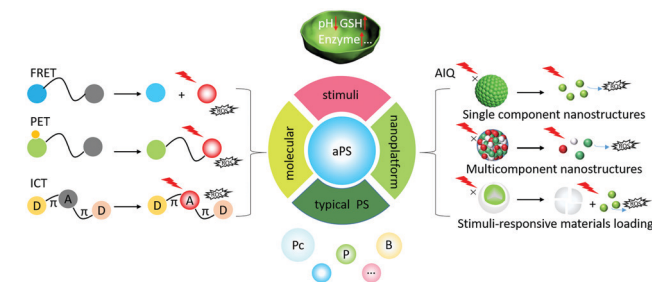
Xingshu Li

cellular microenvironment, acquiring an electron or hydrogen atom to form radicals, including hydroxyl radicals, superoxide ions and hydrogen peroxide. The Type II mechanism transfers the excited triplet state's energy to surrounding oxygen atoms to form singlet oxygen ($^1O_2$).[22,23] ROS can lead directly to cell apoptosis or necrosis,[24,25] and may cause blood vessel damage, leading to hypoxia or starvation.[26,27] They can also cause inflammation and immune effects.[28,29]

1.2 Potential PDT disadvantages

Although PDT has many advantages when compared to conventional chemotherapy and radiotherapy,[30,31] there are still some drawbacks. Currently, PDT is an underutilized clinical treatment and mostly used to treat surficial cancer due to light penetration depth limitations; propagating light through tissue is challenging. Second, current PSs generate ROS mainly *via* the Type II mechanism, which requires a dependence on oxygen. A tumor's hypoxic environment is a major obstacle for this oxygen dependence.[32–34] Last, PSs are always in a turned on state. This is a hindrance as it means they can produce ROS anywhere they are exposed to light irradiation and cannot distinguish between normal tissue and lesion sites, resulting in poor selectivity and relatively high toxicity. As a result, patients receiving PDT need to stay out of light during and after treatment to avoid side effects. This is a great inconvenience.[35,36]

1.3 Activatable photosensitizer (aPS) significance

Traditional PSs are always in an "on" state, which limits PDT's clinical applications. Activatable photosensitizers (aPSs) can remain in an "off" state in healthy tissue, but be activated in carcinoma or diseased sites.[37,38] Pathological sites' microenvironments are different from normal tissues due to rapid metabolic oxidation. They can exhibit higher glutathione (GSH) concentrations, lower pHs, enzyme overexpression, and hypoxia.[39–43] aPSs are designed to respond to neoplastic-associated endogenous stimuli

Scheme 1 Schematic illustration of design strategies including molecular and nanoplatform structures, stimuli and typical PSs for aPSs. B is Boron-dipyrromethene, Pc is phthalocyanine and P is porphyrin.

such as pH, enzyme presence, and GSH concentration.[44–46] aPSs designed with cancer-specific endogenous stimuli responses improve PDT's precision and efficiency for tumor eradication. They work by controlling the PSs' spatiotemporal activation, which decreases the likelihood of side effects to healthy tissues.[47,48] aPSs that respond to biomarkers for tumors and other diseases are of great significance for cancer treatment.

In 2017, we published a summary describing aPS designs that introduced aPSs based on molecular structures.[49] In this review, we describe recent aPS molecule structure developments and introduce aPS nano-engineered supramolecular structures. The emphasis is laid on the design strategies such as förster resonance energy transfer (FRET), intramolecular charge transfer (ICT), photo-induced electron transfer (PET), and aggregation-induced quenching (AIQ). We provide a representative aPS response to tumor-related stimuli (pH, enzyme, and GSH) using these new strategies and advanced aPS applications based on Boron-dipyrromethenes (BODIPYs), Porphyrins (Ps), and Phthalocyanines (Pcs) (Scheme 1). Finally, we also include aPS defects and perspectives.

2 aPS design strategies

aPSs are constructed following numerous conventional design strategies including FRET, ICT, PET, and AIQ.[50,51] There are several other emerging aPS development methods such as PS conjugated structure changes, morphological reorganization and oxygen isolation.[52–54]

2.1 Engineering molecular structures

Using chemical design, PS structures can modulate ROS generation by modifying functional groups (*e.g.* amines and phenolic subunits) and connecting quenchers using response linkers (*e.g.* esters and disulfide linkages).[55–58] Therefore, aPSs responsive to diverse stimuli are created based on the molecular design of different PSs.

2.1.1 pH activation. Tumor site pHs are lower than normal tissues due to hypoxic anaerobic glycolysis.[59–61] This provides a good opportunity to activate PSs after targeting the node.[62]

PET, where the molecular system uses a spacer to connect a fluorophore and an electron donor, is often harnessed for probe molecule design. When it binds to the guest molecule,

Juyoung Yoon received his PhD (1994) from The Ohio State University. After completing postdoctoral research at UCLA and at Scripps Research Institute, he joined the faculty at Silla University in 1998. In 2002, he moved to Ewha Womans University, where he is currently a professor of department of chemistry and nanoscience. He is a member of Korean Academy of Science and Technology, Fellow of the Royal Society of Chemistry and currently a Distinguished Professor of Ewha. He has authored 385 papers with 41 000 total citation with h-index of 103. His research interests include investigations of fluorescent probes, theranostics and organic functional materials.
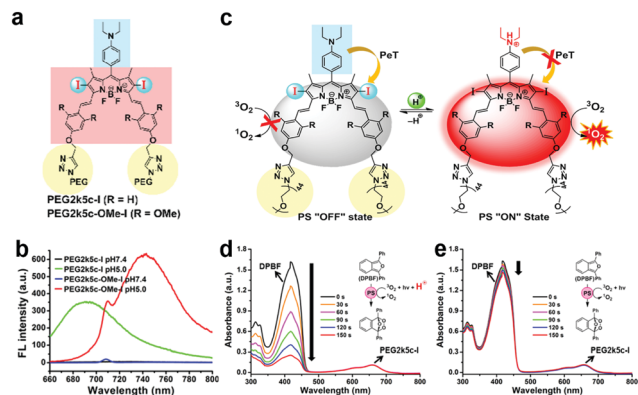
Juyoung Yoon

Fig. 1 (a) PEG2k5c-I and PEG2k5c-OMe-I chemical structures. (b) PEG2k5c-I and PEG2k5c-OMe-I fluorescence spectra under different pHs. (c) Schematic illustration of pH-activatable PSs based on BODIPY. PEG2k5c-I $^1O_2$ generation with (d) and without (e) 0.1% trifluoroacetic acid. Reproduced with permission from ref. 63. Copyright 2018 American Chemical Society.

Fig. 2 (a) Schematic mechanism for cathepsin B activation. (b) Fluorescence spectra (unmodified Pc-COOH as the control). (c) Pc-FcQ and N-Pc-FcQ cell viability treated with HepG2 cells with and without light irradiation. (d) Fluorescence images of tumor-bearing mice injected with Pc-FcQ or N-Pc-FcQ. Reproduced with permission from ref. 68. Copyright 2019 Elsevier.

the PET is inhibited or blocked completely and the fluorophore emits fluorescence for detection. Inspired by this, many pH-triggered aPSs are designed using this mechanism. The most common strategy is to leverage an amine species' protonation and block PET with a pH change. Siegwart and co-workers successfully developed pH-responsive aPSs based on this strategy.[63] They connected tetramethyl-BODIPY (the core scaffold) with a diethylaminophenyl moiety. This rendered PET feasible and gained PEG2k5c-I and PEG2k5c-OMe-I (Fig. 1a). The two molecules remain passive at a normal pH, but are activated in acidic pHs (Fig. 1b). This is attributed to the amino group's protonation under acidic conditions neutralizing the PET process (Fig. 1c). Using 1,3-diphenylisobenzofuran (DPBF), the $^1O_2$ indicator tested whether these two molecules could generate $^1O_2$. Only in the acidic solution was DPBF absorption diminished; it remained unaltered in the neutral solution (Fig. 1d and e), proving that lower pH can activate PS ROS efficiency. There are several aPS studies about PET-capable amino groups.[57,64,65]

In addition to amino groups, Resch-Genger and co-workers prepared a pH-responsive aPS via introducing a meso-substituted phenolic subunit into BODIPYs.[66] The phenolic subunit's deprotonated form deactivates BODIPYs photo-properties due to PET. At the same time, it enables a better Pka due to the tunability for phenolic moieties, which was beneficial for the treatment of various special cells.

2.1.2 Enzyme activation. Enzymes are crucial cellular system biocatalysts. Nodes and diseases are often associated with certain enzyme overexpression. This phenomenon can be exploited for aPS construction.[67]

Enzyme responsive aPSs are created conjugating a quencher and PS through an enzyme-cleavable linker. The PS energy is transferred to the quencher but gets separated after enzyme interaction and is activated. Lo and colleagues reported a cathepsin B-responsive aPS (Pc-FcQ) utilizing a ferrocenyl BODIPY as a dark quencher connected to zinc(II) Pc through a cathepsin B-cleavable linker [Gly-Phe-Leu-Gly-Lys].[68] The ferrocenyl BODIPY's broad

absorption matched the Pc emission and quenched the Pc's photo-activity through FRET. Due to PET, ferrocenyl BODIPY itself had insignificant fluorescence. Fig. 2a shows that Pc-FcQ's optical properties, including fluorescence and ROS generation, were deactivated. Cathepsin B separated BODIPY from PS, eliminated the intramolecular energy conversion, and restored Pc's original photo properties. To better illustrate Pc-FcQ's cathespin B-responsive activity, they prepared N-Pc-FcQ, another non-cleavable control. Both Pc-FcQ and N-Pc-FcQ fluorescence diminished significantly (Fig. 2b). Without light irradiation these two compounds are non-cytotoxic. Upon light irradiation, Pc-FcQ cytotoxicity against HepG2 cells increases because the cathepsin B cleaves the linker and separates Pc and ferrocenyl BODIPY, inducing ROS generation (Fig. 2c). They examined in vivo fluorescence imaging to verify Pc-FcQ activation. Compared to N-Pc-FcQ, Pc-FcQ's fluorescence intensity in tumors reached a plateau after 10 h while N-Pc-FcQ's fluorescence intensity remained weak (Fig. 2d).

PET is also pivotal for enzyme activation. There is a quinone qxidoreductase 1 (hNQO1) aPS based on PET.[69] hNQO1 is overexpressed in many types of cancer cells, making it an ideal candidate. Beharry and co-author incorporated the quinone into phenalenone (PN) (as the PS) through the central amide bond. The electron-deficient quinone quenched PN's optical properties via the PET mechanism and left the aPS in an "off" state in healthy tissue. When hNQO1 was introduced, the quinone underwent intramolecular cyclization, released native PN and restored its photo-activity.

2.1.3 GSH activation. GSH is a small peptide consisting of three amino acids (cysteine, glutamine and glycine). It is an important antioxidant and free radical scavenger in the body. GSH concentration in a tumor site is much higher than in normal cells and extracellular fluid,[70] making GSH a good trigger for aPSs.

Similar to the enzyme response, one design approach is to introduce disulfide bonds. Ng et al. synthesized a series of dendritic Pcs (dimeric, trimeric, and tetrameric PCs) through disulphide bridges.[71] Due to FRET, the fluorescence intensity and ROS generation decreased as more Pc units conjugated. After reacting with GSH, the compounds activated and exhibited high photocytotoxicity. Other studies also used disulfides as
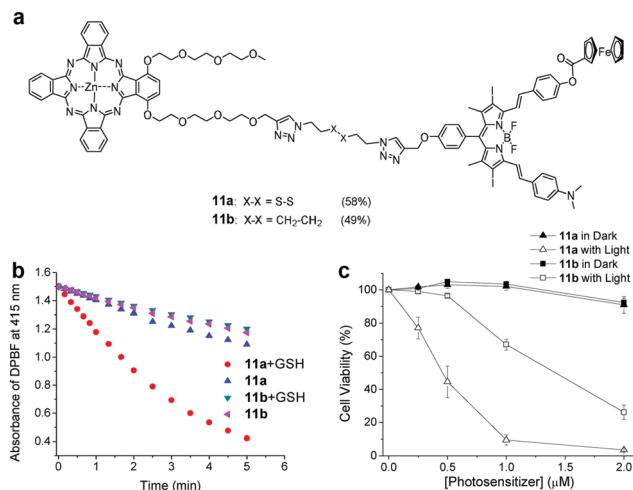
Fig. 3 (a) aPS 11a chemical structure and the non-cleavable control compound 11b. (b) 11a and 11b ROS generation with a DPBF probe. (c) 11a and 11b cell viability with and without light irradiation. Reproduced with permission from ref. 72. Copyright 2019 John Wiley and Sons.

linkers involving FRET.[72] Lo *et al.* linked the photosensitizing unit (zinc(II) Pc) to a BODIPY unit to obtain the GSH-response aPS (11a) while 11b (the non-cleavable analogue) was used as the control (Fig. 3a).[72] They used DPBF as the ROS probe to verify GSH's effect on 11a's ROS generation. The results showed that GSH-treated 11a had a high ROS generation efficiency from cleaved disulphide linkages detaching the quencher from the PSs (Fig. 3b). This is consistent with 11a and 11b cell results (Fig. 3c).

2.1.4 Other activation. Hydrogen peroxide (H_2O_2)-responsive aPS has also been developed.[73] Xing *et al.* synthesized a H_2O_2-responsive pro-PS MBPB by bonding PS methylene blue (MB) with a *p*-phenylboronic ester (PB) *via* a carbonochloridate PB–Cl. The MB conjugation system was destroyed, resulting in the complete disappearance of its photoactivity. MBPB can be activated by H_2O_2 to generate MB and quinone methide (QM). When reacted with H_2O_2, boronic ester oxidation releases QM allowing free MB to produce $^1O_2$ through a rapid 1,6-elimination. They examined the H_2O_2 response using spectroscopy. Due to the MB breakdown, MBPB has no color and no absorption or emissions from 500 nm to 800 nm. Absorption and emissions gradually increase with GSH addition and the solution turns a cyan color.

ICT can affect some fluorophores' absorption bands and aPSs have been established using this strategy. Li and coworkers synthesized a D–π–A PS with a phenolic group electron-donation ability.[74] They used an alkaline phosphatase (ALP) activatable derivative to protect the phenolic hydroxyl and diminish its electron-donating ability. This enabled ICT process suppression and the absorbance at certain wavelengths to disappear. Upon adding ALP, the aPSs restored the absorption band at 616 nm and generated $^1O_2$.

2.2 Nanoengineering supramolecular structures

Most traditional PSs tend to aggregate due to poor water solubility. This impedes their application. Nano-engineered supramolecular

structures improve PS solubility, enhance permeability and retention effects,[75,76] and alter the optical properties, which plays critical roles in exploiting aPSs.

Biological self-assembly through noncovalent interaction[77–79] (hydrophobic, hydrogen-bonding, electrostatic, π–π stacking and van der Waals force interactions) is pervasive in nature. Because of weak and dynamic noncovalent interactions, nano-engineered supramolecular structures can be altered by external stimuli at a low energy cost.

2.2.1 Single component self-assembled nanostructures. Many nano-aPSs self-assemble using a single component based on single chemical modification molecules. Sensitive linkers like disulfides connect hydrophobic PSs with hydrophilic segments to obtain amphiphilic molecular segments (PS-cleaving linker-hydrophilic segments). These are necessary for self-assembly. These nano systems possess passive ("off") states in normal tissue, but switch "on" when exposed to a tumor's overexpressed stimuli.

Choi *et al.* developed a redox-responsive nanogel based on attaching Chlorin e6 (Ce6) to fucoidan using disulfide.[80] Ce6's hydrophobicity allowed a Ce6–fucoidan conjugate to form nanogels through self-assembly. The Ce6 aggregation kept it inactive due to its self-quenching effect. When it reacted with the redox potential, it released Ce6 and photo activity resumed. Fucoidan not only has anticancer potential, but also targets P-selectin, which is overexpressed on some tumor cells' surfaces. Nanogels based on Ce6-fucoidan could reach these lesion sites and enhance the PDT.

Qian and co-workers also reported a redox-activatable nanoparticle.[81] They chemically conjugated Ce6 with hyaluronic acid (HA) through disulfide linkages to obtain HSC conjugates (Ce6-ss-HA) which assembled into nanoparticles (HSC) (Fig. 4a). To enhance PDT's efficiency under hypoxia, they encapsulated perfluorohexane (PFH) in HSC and obtained PFH@HSC. PFH is a perfluorocarbon (PFC), and has an extremely high oxygen solubility. This means that it can provide sufficient oxygen during PDT.[82–84] The disulfide bonds give the molecule reduction-responsive
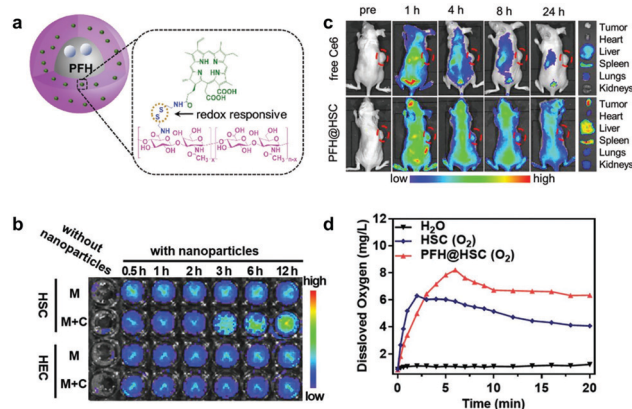

Fig. 4 (a) Schematic illustration of PFH@HSC nanoparticles. (b) NIR images of HSC and HEC nanoparticles treated without (M) and with MDA-MB-231 cells (M + C). (c) *In vivo* fluorescence images. (d) Dissolved oxygen of HSC and PFH@HSC nanoparticles. Reproduced with permission from ref. 81. Copyright 2019 John Wiley and Sons.

1686 | *Mater. Chem. Front.*, 2021, **5**, 1683–1693

This journal is © The Royal Society of Chemistry and the Chinese Chemical Society 2021

switch capability. The nanosystem's phototoxicity remains inert (the "off" state) during blood circulation because of Ce6's AIQ. When the nanoparticles release Ce6 molecules, it restores their fluorescence emission and $^1O_2$ production because of the tumor's relatively high GSH. This was verified by time-dependent HSC nanoparticles co-incubated with MDA-MB-231 fluorescence recovery (Fig. 4b). In contrast to free Ce6's rapid blood clearance, PFH@HSC nanoparticles concentrated in tumor sites 4 h post-injection from fluorescence imaging (Fig. 4c). Compared to HSC, PFH@HSC demonstrated excellent oxygen loading and gradual release capability (Fig. 4d). To detect tumor oxygen levels, they carried out *in vivo* photoacoustic (PA) imaging and *ex vivo* immunofluorescence staining. PA imaging verified that higher oxyhemoglobin intensity was enhanced by PFH@HSC nanoparticles due to oxyhemoglobin and deoxyhemoglobin's diverse absorption spectra. Compared to control groups, the *in vivo* results demonstrated PFH@HSC nanoparticles' tumor inhibition capabilities.

There are several amphipathic PSs without sensitive linkers that can self-assemble into stable nanostructures. Disassembly can occur from biomarker presence rather than intermolecular forces.[85,86] We developed a series of aPSs based on Pcs, which act as described above.[6,87–92] Among these aPSs, one self-assembles building blocks (Pc-4TEG) that consist of zinc(II) Pc modified with the hydrophilic moiety triethylene glycol (TEG) (biotin).[87] The hydroxyl group terminal allows a biotin substitution for the PS (Pc-4TEG-B) target (Fig. 5a). Pc-4TEG-B's amphiphilic structure makes it feasible to form a stable nanostructure (NanoPcTB). NanoPcTB's fluorescence was completely quenched in water (Fig. 5b). We chose avidin as the targeted protein to demonstrate its protein-responsive properties. Upon adding the avidin, NanoPcTB's fluorescence increased. There was no significant fluorescence increase when we incubated NanoPcTB with extra biotin prior to adding avidin (Fig. 5c). Fluorescence did not increase for NanoPcT after adding avidin. We tested a variety of proteins but only the avidin turned on fluorescence. This demonstrates NanoPcTB's high avidin selectivity (Fig. 5d). Avidin addition significantly restored ROS

generation (Fig. 5e). All of our results verified NanoPcTB's excellent ability to switch its photosensitivity. This is significant for PDT.

Our research group[92] also reported on a "one-for-all" switchable nanotheranostic (NanoPcS) utilizing an amphiphilic Pc derivative as the building block. This NanoPcS forms uniform nanovesicles dispersed in an aqueous solution. The NanoPcS's photo-properties are sustained in an "off" state due to AIQ, but turn "on" fluorescence and ROS generation in the presence of protein. More significantly, we confirmed specific binding between albumin and the Pc molecule using an inducible transgenic mouse system.

Morphological rearrangements based on tumor-associated stimuli can also activate optical properties. Hest and coworkers developed an acid-activatable nanomaterial based on a peptide–porphyrin conjugate (PWG) synthesized using a pH-responsive dipeptide tryptophan-glycine (WG) and a hydrophobic porphyrin (P).[93] They obtained stable nanoparticles using PWG in a normal physiological environment. The nanomaterial transformed into nanofibers in acidic solutions because of the stronger inter-molecular hydrogen bonds from PWG protonation (Fig. 6a). To evaluate pH effects on the PWG nanostructures' photoactivity, they used a 9,10-anthracenediyl-bis(methylene)dimalonic acid (ABDA) probe to test $^1O_2$ generation. The lower the pH, the higher the $^1O_2$ generation. This indicates that the acidic environment enhances ROS production (Fig. 6b). The structural transformation also led to long-term retention and excellent anti-tumor efficiency.

2.2.2 Multicomponent co-assembled nanostructures. Although single component self-assembly performs well when constructing aPSs, there are several obstacles during its clinical transformation. These include complicated molecular design, tedious synthesis processes, and photochemical property changes due to moiety introduction.[94] We utilized molecular recognition interactions (π–π stacking and electrostatic interactions) between zinc(II) Pc tetra substituted with 6,8-disulfonate-2-naphthyloxy groups (PcS) and the anticancer drug mitoxantrone (MA) to prepare uniform nanoparticles (PcS-MA) in water.[6] These nanoparticles disassembled when reacted with nucleic acids (Fig. 7a). Aggregation quenching led PcS-MA has almost no fluorescence emission, which is consistent with its lack of $^1O_2$ generation (Fig. 7b and c). Adding DNA caused an increase in the PcS-MA's $^1O_2$ generation and fluorescence
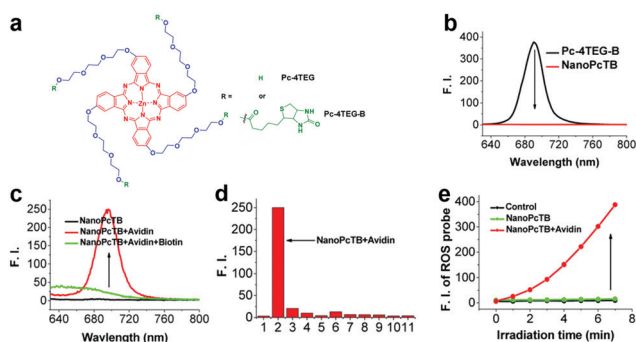

Fig. 5 (a) Chemical structures of Pc-4TEG and Pc-4TEG-B. (b) Fluorescence spectra of Pc-4TEG-B and NanoPcTB. (c) NanoPcTB fluorescence spectra with different treatments. (d) NanoPcTB fluorescence intensity changes when treated with different proteins. (e) NanoPcTB ROS generation without and with avidin. Reproduced with permission from ref. 87. Copyrights 2017 American Chemical Society.
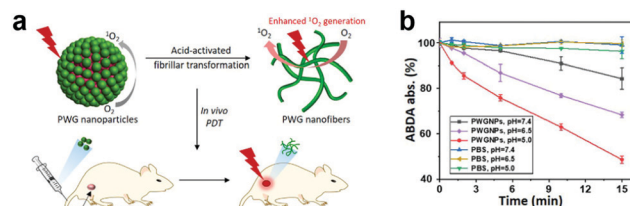

Fig. 6 (a) Schematic illustration of PWG transformation from nanoparticles to nanofibers. (b) PWGNP's single oxygen generation for various pHs. Reproduced with permission from ref. 93. Copyright 2020 John Wiley and Sons.

This journal is © The Royal Society of Chemistry and the Chinese Chemical Society 2021

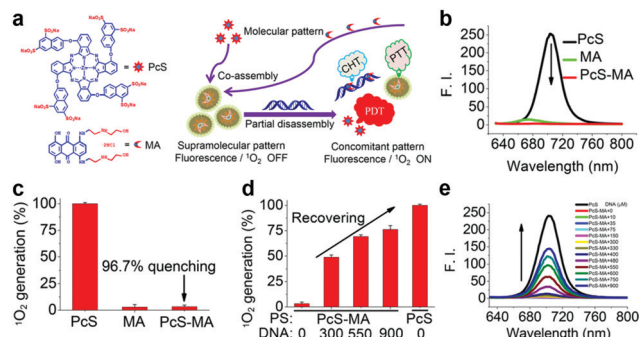*Mater. Chem. Front.*, 2021, **5**, 1683–1693 | **1687**

Fig. 7 (a) PcS and MA chemical structure and schematic illustration of nanoparticle preparation. PcS, MA and PcS-MA comparison of (b) fluorescence and (c) $^1O_2$ generation. PcS-MA (d) $^1O_2$ generation and (e) fluorescence change with ctDNA addition. Reproduced with permission from ref. 6. Copyrights 2018 American Chemical Society.

Fig. 9 (a) Schematic illustration of metallo-nanodrugs coordinated by peptides, PSs and zinc ions. Schematic illustration and pictures of nano-particle (Fmoc-H/Zn^{2+} and Z-HF/Zn^{2+}) response to (b) pH and (c) GSH. (d) Ce6 release under different conditions. (e) Tumor growth with different treatments. Reproduced with permission from ref. 99. Copyright 2018 American Chemical Society.

(Fig. 7d and e). This could be attributed DNA binding with MA and competes with the MA and PcS interaction, resulting in a partial PcS-MA disassembly.

Besides AIQ for multicomponent co-assembled aPSs, the FRET strategy was also used to construct aPSs.[95] Wang and colleagues reported a mitochondria targeted pH-activatable nanoparticle (M-TPPa) based on FRET.[96] They obtained pH-activatable nanoparticles by co-assembling a mitochondria-targeted PS (TPPa) with a pH responsive fluorescent copolymer (mPEG-b-PDPA-Cy7.5) (Fig. 8a). FRET between TPPa and Cy7.5 molecules quenched TPPs photoactivity. When it reached the tumor site, the photodynamic effect was switched on and enhanced, achieving targeted tumor inhibition. Fluorescence was enhanced at least 111-fold, proving nanoparticle dissolution and activation (Fig. 8b). ROS generation under acidic conditions demonstrates the nanoparticles' pH response (Fig. 8c). To further demonstrate FRET effects, they compared PDPA-Cy7.5@TPPa to PDPA@TPPa. PDPA-Cy7.5@TPPa ROS increased production by 151-fold after FRET effect removal. PDPA@TPPa ROS generation was only enhanced 9-fold (Fig. 8d).

GSH can complex with various metal ions due to its two carboxyl and single thiol groups.[97,98] Yan's group reported a smart metallo-nanodrug based on multicomponent coordination that

responds to pH and GSH.[99] They first obtained the nano-particles (Fmoc-H/Zn^{2+} and Z-HF/Zn^{2+}) using the metal-binding peptide (fluorenylmethoxycarbonyl-L-histidine (Fmoc-H) and N-benzyloxycarbonyl-L-histidine-L-phenylalanine (Z-HF)) coordi-nated with Zn^{2+} (Fig. 9a). They verified pH response by changing the Fmoc-H/Zn^{2+} and Z-HF/Zn^{2+} solution's pH. The solution changed from milky white to transparent at pH lower than 5.0 or higher than 8.5 (Fig. 9b). This is attributed to weakening the histidine/Zn^{2+} complex and hydrophobic interaction, respec-tively. Both induced nanoparticle disassembly. GSH coordinated competitively with Zn^{2+}, which caused nanoparticle collapse (Fig. 9c). Ce6 was selected to coordinate cooperatively with Fmoc-H or Z-HF and Zn^{2+} to prepare the metallo-nanodrugs (Fmoc-H/Zn^{2+}/Ce6 or Z-HF/Zn^{2+}/Ce6). Ce6 release detection under dissimilar conditions showed that Fmoc-H/Zn^{2+}/Ce6 remained stable under physiological conditions for a long time, and released explosively at lower pHs or in the presence of GSH (Fig. 9d). Compared to un-encapsulated Ce6, the metallo-nanodrugs significantly enhanced the therapeutic effect (Fig. 9e).

Yan et al. also developed a GSH responsive multifunctional theranostic nanoplatform coordinated by the amphiphilic amino acid (Fmoc-L-L), Mn^{2+} as a magnetic resonance imaging (MRI) contrast agent and a photosensitive drug (chlorin e6, Ce6).[100] The biometal–organic nanoparticles enhanced PDT via efficiently delivering PSs to the nidus region and releasing them through GSH's competitive coordination with Mn^{2+}.

2.2.3 Other supramolecular structures. Another common strategy for constructing aPSs is to take advantage of loading PSs with materials sensitive to tumor-relevant stimuli. Liu et al. designed a GSH-responsive PS based on a Cu(II) Metal–Organic Framework (MOF).[52] They loaded PS into the pores of a suitable MOF to isolate the PS from O_2, which resulted in inhibiting ROS production. Given that redox-active metal like Cu(II) can be oxidized by GSH, the MOFs dissociated and released PSs upon reacting with GSH. When the PSs came into contact with oxygen they generated ROS with suitable light irradiation. Other MOF aPSs have also been reported.[101,102]

Fig. 8 (a) Schematic illustration of pH-activatable nanoparticle M-TPPa. (b) Cy7.5 fluorescence and TPPa response to different pHs. (c) M-TPPa ROS generation at different pHs. (d) ROS generation comparison before and after pH response in PDPA-Cy7.5@TPPa and PDPA@TPPa. Reproduced with permission from ref. 96. Copyright 2019 Elsevier.

1688 | Mater. Chem. Front., 2021, **5**, 1683–1693

This journal is © The Royal Society of Chemistry and the Chinese Chemical Society 2021
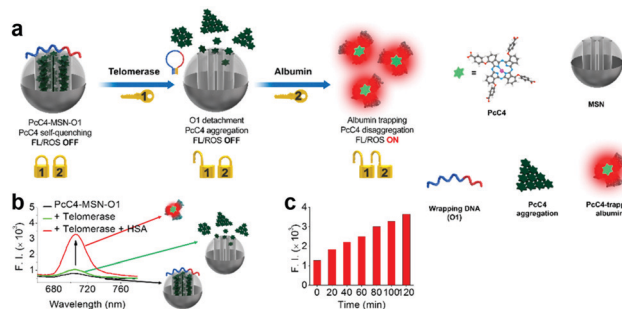
Fig. 10 (a) Schematic illustration sequential protein-responsive PcC4-MSN-O1 activation. (b) Fluorescence spectra of PcC4-MSN-O1, PcC4-MSN-O1 treated with telomerase and PcC4-MSN-O1 co-treated with telomerase and HSA. (c) Fluorescence intensity of PcC4-MSN-O1 treated with telomerase for different times then incubated with HSA for 10 min. Reproduced with permission from ref. 91. Copyrights 2019 American Chemical Society.

Our group developed a sequential protein-responsive aPS (PcC4-MSN-O1) using mesoporous silica nanoparticles (MSNs) to load PS.[91] Because carboxy-terminal zinc(ii) Pcs interact strongly with albumin,[85,86] we selected zinc(ii) Pc tetra-α-substituted with 4-carboxylphenoxy groups (PcC4) as the model PS. To further enhance tumor-specificity accuracy, we loaded PcC4 with mesoporous silica nanoparticles (MSNs) and sealed them with a telomerase-responsive DNA O1 through strong electrostatic interactions (Fig. 10a). The quenched fluorescence was successfully restored by telomerase and albumin stimulation response (Fig. 10b). To further demonstrate MSNs encapsulating PS significance, we incubated PcC4-MSN-O1 with telomerase for different lengths of time followed by a 10 min HSA incubation (Fig. 10c). The increasing fluorescence intensity indicates that telomerase plays an important role in PcC4's photo-activity recovery.

Macrocyclic molecules are regarded as a special carrier for PS delivery. Macrocyclic molecules like cyclodextrins (CDs), calixarenes (CAs), and crown ethers have a large cavity that selectively encapsulates the guest molecule through weak interaction.[103] There are many studies based on this structure, where PSs are loaded into macrocyclic molecules to achieve aPSs. The interaction of PSs in the cavity leads to photoactivity loss, while the over-expressed biomarkers release PSs through competition with the macrocyclic molecules. Guo and co-workers used guanidinium-modified calix[5]arene pentadodecyl ether (GC5A-12C) as the macrocyclic amphiphile vector, which has a high PS and adenosine triphosphate (ATP) affinity.[94] They

preloaded the PS into GC5A-12C making it nontoxic for blood circulation. In the presence of ATP, the stronger bonding between GC5A-12C and ATP releases the PSs and leads to fluorescence and ROS generation recovery (Fig. 11).

3 Conclusions and outlook

Molecular structures based on various design strategies and nanoengineered supramolecular structures assembled from a variety of components all exhibit excellent aPS activating properties when exposed to tumor-related stimulants such as pH, enzymes, and GSH. This work is a major stride forward in precision treatment of nodes. There are still several challenges to be addressed, however.

To some extent, biological safety was ignored in nanomaterial aPS preparation. Many reports used doped inorganic heavy metals, which may impact an organism's health. Future biocompatible material research will be more beneficial for clinical transformation. Second, most pH-responsive aPSs are designed to be activated at a low pH (5.0) whereas endosomes and lysosomes in normal intracellular tissue also have low pH's (5.0–6.5 and 4.5–5.0, respectively).[104,105] For this kind of aPS, being able to precisely target a lesion site is extremely important. Third, aPS use involves two processes, quenching and activation. There is little research, however, on quenching and reactivation efficiency. aPS quenching and activation efficiency studies require more consideration. Finally, most aPSs have only been verified in response to stimuli *in vitro*; further *in vivo* activation validation is required. In addition, light's tissue depth penetration and the "Achilles' heels" of tumor-environment hypoxia have seriously hindered PDT's therapeutic effects. These issues also require further exploration.

In general, there is still much effort required for aPS development. We hope that this review provides some meaningful references for future exploration.

Conflicts of interest

There are no conflicts to declare.

Acknowledgements

References

1 J. F. Lovell, C. S. Jin, E. Huynh, H. Jin, C. Kim, J. L. Rubinstein, W. C. W. Chan, W. Cao, L. V. Wang and G. Zheng, Porphysome Nanovesicles Generated by Porphyrin Bilayers for Use as Multimodal Biophotonic Contrast Agents, *Nat. Mater.*, 2011, **10**, 324–332.
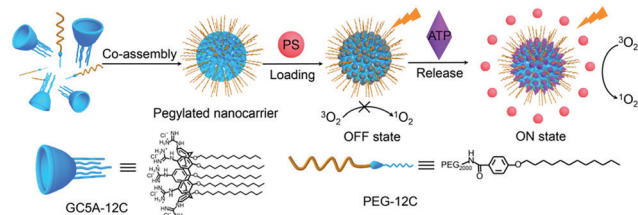

Fig. 11 Schematic illustration of aPSs based on the pegylated GC5A-12C as the PS nanocarrier. Reproduced with permission from ref. 94. Copyrights 2018 American Chemical Society.

2 K. M. Harmatys, M. Overchuk and G. Zheng, Rational Design of Photosynthesis-Inspired Nanomedicines, *Acc. Chem. Res.*, 2019, **52**, 1265–1274.

3 J. Meulemans, P. Delaere and V. Vander Poorten, Photo-dynamic Therapy in Head and Neck Cancer: Indications, Outcomes, and Future Prospects, *Curr. Opin. Otolaryngol. Head Neck Surg.*, 2019, **27**, 136–141.

4 P. Rai, S. Mallidi, X. Zheng, R. Rahmanzadeh, Y. Mir, S. Elrington, A. Khurshid and T. Hasan, Development and Applications of Photo-Triggered Theranostic Agents, *Adv. Drug Delivery Rev.*, 2010, **62**, 1094–1124.

5 D. W. Felsher, Cancer Revoked: Oncogenes as Therapeutic Targets, *Nat. Rev. Cancer*, 2003, **3**, 375–380.

6 X. Li, S. Yu, D. Lee, G. Kim, B. Lee, Y. Cho, B. Y. Zheng, M. R. Ke, J. D. Huang, K. T. Nam, X. Chen and J. Yoon, Facile Supramolecular Approach to Nucleic-Acid-Driven Activatable Nanotheranostics That Overcome Drawbacks of Photodynamic Therapy, *ACS Nano*, 2018, **12**, 681–688.

7 G. Yang, L. Xu, J. Xu, R. Zhang, G. Song, Y. Chao, L. Feng, F. Han, Z. Dong, B. Li and Z. Liu, Smart Nanoreactors for pH-Responsive Tumor Homing, Mitochondria-Targeting, and Enhanced Photodynamic-Immunotherapy of Cancer, *Nano Lett.*, 2018, **18**, 2475–2484.

8 H. Koo, H. Lee, S. Lee, K. H. Min, M. S. Kim, D. S. Lee, Y. Choi, I. C. Kwon, K. Kim and S. Y. Jeong, *In Vivo* Tumor Diagnosis and Photodynamic Therapy via Tumoral pH-Responsive Polymeric Micelles, *Chem. Commun.*, 2010, **46**, 5668–5670.

9 J. P. Celli, B. Q. Spring, I. Rizvi, C. L. Evans, K. S. Samkoe, S. Verma, B. W. Pogue and T. Hasan, Imaging and Photo-dynamic Therapy: Mechanisms, Monitoring, and Optimization, *Chem. Rev.*, 2010, **110**, 2795–2838.

10 B. M. Luby, C. D. Walsh and G. Zheng, Advanced Photo-sensitizer Activation Strategies for Smarter Photodynamic Therapy Beacons, *Angew. Chem., Int. Ed.*, 2019, **58**, 2558–2569.

11 T. J. Dougherty, C. J. Gomer, B. W. Henderson, G. Jori, D. Kessel, M. Korbelik, J. Moan and Q. Peng, Photody-namic Therapy, *J. Natl. Cancer Inst.*, 1998, **90**, 889–905.

12 X. Li, S. Lee and J. Yoon, Supramolecular Photosensitizers Rejuvenate Photodynamic Therapy, *Chem. Soc. Rev.*, 2018, **47**, 1174–1188.

13 T. J. Dougherty, J. E. Kaufman, A. Goldfarb, K. R. Weishaupt, D. Boyle and A. Mittleman, Photoradiation Therapy for the Treatment of Malignant Tumors, *Cancer Res.*, 1978, **38**, 2628–2635.

14 K. Plaetzer, B. Krammer, J. Berlanda, F. Berr and T. Kiesslich, Photophysics and Photochemistry of Photodynamic Therapy: Fundamental Aspects, *Lasers Med. Sci.*, 2009, **24**, 259–268.

15 P. Huang, Z. Li, J. Lin, D. Yang, G. Gao, C. Xu, L. Bao, C. Zhang, K. Wang, H. Song, H. Hu and D. Cui, Photosensitizer-Conjugated Magnetic Nanoparticles for *in Vivo* Simulta-neous Magnetofluorescent Imaging and Targeting Therapy, *Biomaterials*, 2011, **32**, 3447–3458.

16 W. M. Sharman, J. E. van Lier and C. M. Allen, Targeted Photodynamic Therapy via Receptor Mediated Delivery Systems, *Adv. Drug Delivery Rev.*, 2004, **56**, 53–76.

17 B. D. Zheng, Q. X. He, X. Li, J. Yoon and J.-D. Huang, Phthalocyanines as Contrast Agents for Photothermal Therapy, *Coord. Chem. Rev.*, 2021, **426**, 213548.

18 J. F. Lovell, T. W. B. Liu, J. Chen and G. Zheng, Activatable Photosensitizers for Imaging and Therapy, *Chem. Rev.*, 2010, **110**, 2839–2857.

19 X. Li, B. D. Zheng, X. H. Peng, S. Z. Li, J. W. Ying, Y. Zhao, J. D. Huang and J. Yoon, Phthalocyanines as Medicinal Photosensitizers: Developments in the Last Five Years, *Coord. Chem. Rev.*, 2019, **379**, 147–160.

20 M. Triesscheijn, P. Baas, J. H. Schellens and F. A. Stewart, Photodynamic Therapy in Oncology, *Oncologist*, 2006, **11**, 1034–1044.

21 C. S. Foote, Definition of Type I and Type II Photosensitized Oxidation, *Photochem. Photobiol.*, 1991, **54**, 659.

22 D. van Straten, V. Mashayekhi, H. S. de Bruijn, S. Oliveira and D. J. Robinson, Oncologic Photodynamic Therapy: Basic Principles, Current Clinical Status and Future Directions, *Cancers*, 2017, **9**, 19.

23 P. Agostinis, K. Berg, K. A. Cengel, T. H. Foster, A. W. Girotti, S. O. Gollnick, S. M. Hahn, M. R. Hamblin, A. Juzeniene, D. Kessel, M. Korbelik, J. Moan, P. Mroz, D. Nowis, J. Piette, B. C. Wilson and J. Golab, Photodynamic Therapy of Cancer: An Update, *Ca-Cancer J. Clin.*, 2011, **61**, 250–281.

24 N. L. Oleinick, R. L. Morris and I. Belichenko, The Role of Apoptosis in Response to Photodynamic Therapy: What, Where, Why, and How, *Photochem. Photobiol. Sci.*, 2002, **1**, 1–21.

25 E. Buytaert, M. Dewaele and P. Agostinis, Molecular Effec-tors of Multiple Cell Death Pathways Initiated by Photo-dynamic Therapy, *Biochim. Biophys. Acta*, 1776, **2007**, 86–107.

26 D. E. J. G. J. Dolmans, A. Kadambi, J. S. Hill, C. A. Waters, B. C. Robinson, J. P. Walker, D. Fukumura and R. K. Jain, Vascular Accumulation of a Novel Photosensitizer, MV6401, Causes Selective Thrombosis in Tumor Vessels after Photo-dynamic Therapy, *Cancer Res.*, 2002, **62**, 2151–2156.

27 V. H. Fingar, Vascular Effects of Photodynamic Therapy, *J. Clin. Laser Med. Surg.*, 1996, **14**, 323–328.

28 A. P. Castano, P. Mroz and M. R. Hamblin, Photodynamic Therapy and Anti-Tumour Immunity, *Nat. Rev. Cancer*, 2006, **6**, 535–545.

29 A. D. Garg, D. V. Krysko, T. Verfaillie, A. Kaczmarek, G. B. Ferreira, T. Marysael, N. Rubio, M. Firczuk, C. Mathieu, A. J. M. Roebroek, W. Annaert, J. Golab, P. de Witte, P. Vandenabeele and P. Agostinis, A Novel Pathway Combining Calreticulin Exposure and ATP Secretion in Immunogenic Cancer Cell Death, *EMBO J.*, 2012, **31**, 1062–1079.

30 S. Kim, T. Y. Ohulchanskyy, H. E. Pudavar, R. K. Pandey and P. N. Prasad, Organically Modified Silica Nano-particles Co-encapsulating Photosensitizing Drug and Aggregation-Enhanced Two-Photon Absorbing Fluorescent Dye Aggregates for Two-Photon Photodynamic Therapy, *J. Am. Chem. Soc.*, 2007, **129**, 2669–2675.

31 W. P. Hogle, The State of the Art in Radiation Therapy, *Semin. Oncol. Nurs.*, 2006, **22**, 212–220.

32 M. Li, J. Xia, R. Tian, J. Wang, J. Fan, J. Du, S. Long, X. Song, J. W. Foley and X. Peng, Near-Infrared Light-Initiated Molecular Superoxide Radical Generator: Rejuvenating Photodynamic Therapy against Hypoxic Tumors, *J. Am. Chem. Soc.*, 2018, **140**, 14851–14859.

33 Z. Zhou, J. Song, L. Nie and X. Chen, Reactive Oxygen Species Generating Systems Meeting Challenges of Photodynamic Cancer Therapy, *Chem. Soc. Rev.*, 2016, **45**, 6597–6626.

34 V. Catalano, A. Turdo, S. Di Franco, F. Dieli, M. Todaro and G. Stassi, Tumor and Its Microenvironment: A Synergistic Interplay, *Semin. Cancer Biol.*, 2013, **23**, 522–532.

35 Z. Huang, A Review of Progress in Clinical Photodynamic Therapy, *Technol. Cancer Res. Treat.*, 2005, **4**, 283–293.

36 Y. Wang, Y. Lin, H. G. Zhang and J. Zhu, A Photodynamic Therapy Combined with Topical 5-Aminolevulinic Acid and Systemic Hematoporphyrin Derivative is More Efficient but Less Phototoxic for Cancer, *J. Cancer Res. Clin. Oncol.*, 2016, **142**, 813–821.

37 P. Cheng and K. Pu, Activatable Phototheranostic Materials for Imaging-Guided Cancer Therapy, *ACS Appl. Mater. Interfaces*, 2020, **12**, 5286–5299.

38 G. Yang, C. Chen, Y. Zhu, Z. Liu, Y. Xue, S. Zhong, C. Wang, Y. Gao and W. Zhang, GSH-Activatable NIR Nanoplatform with Mitochondria Targeting for Enhancing Tumor-Specific Therapy, *ACS Appl. Mater. Interfaces*, 2019, **11**, 44961–44969.

39 G. Yang, L. Xu, Y. Chao, J. Xu, X. Sun, Y. Wu, R. Peng and Z. Liu, Hollow MnO_2 as A Tumor-Microenvironment-Responsive Biodegradable Nano-platform for Combination Therapy Favoring Antitumor Immune Responses, *Nat. Commun.*, 2017, **8**, 902.

40 C. H. Chang, J. Qiu, D. O'Sullivan, M. D. Buck, T. Noguchi, J. D. Curtis, Q. Chen, M. Gindin, M. M. Gubin, G. J. van der Windt, E. Tonc, R. D. Schreiber, E. J. Pearce and E. L. Pearce, Metabolic Competition in the Tumor Microenvironment Is a Driver of Cancer Progression, *Cell*, 2015, **162**, 1229–1241.

41 D. F. Quail and J. A. Joyce, Microenvironmental Regulation of Tumor Progression and Metastasis, *Nat. Med.*, 2013, **19**, 1423–1437.

42 M. A. Swartz, N. Iida, E. W. Roberts, S. Sangaletti, M. H. Wong, F. E. Yull, L. M. Coussens and Y. A. DeClerck, Tumor Microenvironment Complexity: Emerging Roles in Cancer Therapy, *Cancer Res.*, 2012, **72**, 2473–2480.

43 S. Li, W. Zhang, H. Xue, R. Xing and X. Yan, Tumor Microenvironment-Oriented Adaptive Nanodrugs Based on Peptide Self-Assembly, *Chem. Sci.*, 2020, **11**, 8644–8656.

44 P. Vaupel, F. Kalliniwski and P. Okunieff, Oxygen and Nutrient Supply, and Metabolic Microenvironment of Human Tumors: A Review, *Cancer Res.*, 1989, **49**, 6449–6465.

45 S. Mura, J. Nicolas and P. Couvreur, Stimuli-Responsive Nanocarriers for Drug Delivery, *Nat. Mater.*, 2013, **12**, 991–1003.

46 R. C. H. Wong, P. C. Lo and D. K. P. Ng, Stimuli Responsive Phthalocyanine-Based Fluorescent Probes and Photosensitizers, *Coord. Chem. Rev.*, 2019, **379**, 30–46.

47 K. Han, S. B. Wang, Q. Lei, J. Y. Zhu and X. Z. Zhang, Ratiometric Biosensor for Aggregation-Induced Emission-Guided Precise Photodynamic Therapy, *ACS Nano*, 2015, **9**, 10268–10277.

48 J. Tian, L. Ding, H. J. Xu, Z. Shen, H. Ju, L. Jia, L. Bao and J. S. Yu, Cell-Specific and pH-Activatable Rubyrin-Loaded Nanoparticles for Highly Selective Near-infrared Photodynamic Therapy Against Cancer, *J. Am. Chem. Soc.*, 2013, **135**, 18850–18858.

49 X. Li, S. Kolemen, J. Yoon and E. U. Akkaya, Activatable Photosensitizers: Agents for Selective Photodynamic Therapy, *Adv. Funct. Mater.*, 2017, **27**, 1604053.

50 J. Bhaumik, R. Weissleder and J. R. McCarthy, Synthesis and Photophysical Properties of Sulfonamidophenyl Porphyrins as Models for Activatable Photosensitizers, *J. Org. Chem.*, 2009, **74**, 5894–5901.

51 P. C. Lo, M. S. Rodriguez-Morgade, R. K. Pandey, D. K. P. Ng, T. Torres and F. Dumoulin, The Unique Features and Promises of Phthalocyanines as Advanced Photosensitisers for Photodynamic Therapy of Cancer, *Chem. Soc. Rev.*, 2020, **49**, 1041–1056.

52 Y. Wang, W. Wu, J. Liu, P. N. Manghnani, F. Hu, D. Ma, C. Teh, B. Wang and B. Liu, Cancer-Cell-Activated Photodynamic Therapy Assisted by Cu(II)-Based Metal-Organic Framework, *ACS Nano*, 2019, **13**, 6879–6890.

53 Z. Wang, Y. Ju, Z. Ali, H. Yin, F. Sheng, J. Lin, B. Wang and Y. Hou, Near-Infrared Light and Tumor Microenvironment Dual Responsive Size-Switchable Nanocapsules for Multimodal Tumor Theranostics, *Nat. Commun.*, 2019, **10**, 4418.

54 M. Li, Y. Ning, J. Chen, X. Duan, N. Song, D. Ding, X. Su and Z. Yu, Proline Isomerization-Regulated Tumor Microenvironment-Adaptable Self-Assembly of Peptides for Enhanced Therapeutic Efficacy, *Nano Lett.*, 2019, **19**, 7965–7976.

55 K. Hirakawa and H. Segawa, Acid Dissociation of the Axial Hydroxyl Group of Hydroxyl(1-pyrenebutoxy)phosphorus(V) Porphyrin Controls the Intramolecular Excitation Energy Transfer, *Photochem. Photobiol. Sci.*, 2010, **9**, 704–709.

56 X. Zhu, W. Lu, Y. Zhang, A. Reed, B. Newton, Z. Fan, H. Yu, P. C. Ray and R. Gao, Imidazole-Modified Porphyrin as A pH-Responsive Sensitizer for Cancer Photodynamic Therapy, *Chem. Commun.*, 2011, **47**, 10311–10313.

57 H. Horiuchi, R. Kuribara, A. Hirabara and T. Okutsu, pH-Response Optimization of Amino-Substituted Tetraphenylporphyrin Derivatives as pH-Activatable Photosensitizers, *J. Phys. Chem. A*, 2016, **120**, 5554–5561.

58 H. Horiuchi, A. Hirabara and T. Okutsu, Importance of the Orthogonal Structure between Porphyrin and Aniline Moieties on the pH-Activatable Porphyrin Derivative for Photodynamic Therapy, *J. Photochem. Photobiol., A*, 2018, **365**, 60–66.

59 G. Helmlinger, A. SCkell, M. Dellian, N. S. Forbes and R. K. Jain, Acid Production in Glycolysis-impaired Tumors Provides New Insights into Tumor Metabolism, *Clin. Cancer Res.*, 2002, **8**, 1284–1291.

60 I. F. Tannock and D. Rotin, Acid pH in Tumors and Its Potential for Therapeutic Exploitation, *Cancer Res.*, 1989, **49**, 4373–4384.

This journal is © The Royal Society of Chemistry and the Chinese Chemical Society 2021

Mater. Chem. Front., 2021, **5**, 1683–1693 | **1691**

61 M. F. Chung, H. Y. Liu, K. J. Lin, W. T. Chia and H. W. Sung, A pH-Responsive Carrier System that Generates NO Bubbles to Trigger Drug Release and Reverse P-Glycoprotein-Mediated Multidrug Resistance, *Angew. Chem., Int. Ed.*, 2015, **54**, 9890–9893.

62 Y. Kato, S. Ozawa, C. Miyamoto, Y. Maehata, A. Suzuki, T. Maeda and Y. Baba, Acidic Extracellular Microenvironment and Cancer, *Cancer Cell Int.*, 2013, **13**, 89.

63 H. Xiong, K. Zhou, Y. Yan, J. B. Miller and D. J. Siegwart, Tumor-Activated Water-Soluble Photosensitizers for Near-Infrared Photodynamic Cancer Therapy, *ACS Appl. Mater. Interfaces*, 2018, **10**, 16335–16343.

64 F. Xue, P. Wei, X. Ge, Y. Zhong, C. Cao, D. Yu and T. Yi, A pH-Responsive Organic Photosensitizer Specifically Activated by Cancer Lysosomes, *Dyes Pigm.*, 2018, **156**, 285–290.

65 M. L. Agazzi, J. E. Durantini, N. S. Gsponer, A. M. Durantini, S. G. Bertolotti and E. N. Durantini, Light-Harvesting Antenna and Proton-Activated Photodynamic Effect of a Novel BODIPY-Fullerene C60 Dyad as Potential Antimicrobial Agent, *ChemPhysChem*, 2019, **20**, 1110–1125.

66 S. Radunz, S. Wedepohl, M. Rohr, M. Calderon, H. R. Tschiche and U. Resch-Genger, pH-Activatable Singlet Oxygen-Generating Boron-dipyrromethenes (BODIPYs) for Photodynamic Therapy and Bioimaging, *J. Med. Chem.*, 2020, **63**, 1699–1708.

67 Y. Choi, R. Weissleder and C.-H. Tung, Selective Antitumor Effect of Novel Protease-Mediated Photodynamic Agent, *Cancer Res.*, 2006, **66**, 7225–7229.

68 Q. Wang, L. Yu, R. C. H. Wong and P.-C. Lo, Construction of Cathepsin B-Responsive Fluorescent Probe and Photosensitizer Using A Ferrocenyl Boron Dipyrromethene Dark Quencher, *Eur. J. Med. Chem.*, 2019, **179**, 828–836.

69 E. M. Digby, O. Sadovski and A. A. Beharry, An Activatable Photosensitizer Targeting Human NAD(P)H: Quinone Oxidoreductase 1, *Chem. – Eur. J.*, 2020, **26**, 2713–2718.

70 G. Pani, T. Galeotti and P. Chiarugi, Metastasis: Cancer Cell's Escape from Oxidative Stress, *Cancer Metastasis Rev.*, 2010, **29**, 351–378.

71 S. Y. S. Chow, R. C. H. Wong, S. Zhao, P. C. Lo and D. K. P. Ng, Disulfide-Linked Dendritic Oligomeric Phthalocyanines as Glutathione-Responsive Photosensitizers for Photodynamic Therapy, *Chemistry*, 2018, **24**, 5779–5789.

72 W. J. Shi, D. K. P. Ng, S. Zhao and P. C. Lo, A Phthalocyanine-Based Glutathione-Activated Photosensitizer with a Ferrocenyl Boron Dipyrromethene Dark Quencher for Photodynamic Therapy, *ChemPhotoChem*, 2019, **3**, 1004–1013.

73 Q. Zeng, R. Zhang, T. Zhang and D. Xing, H_2O_2-Responsive Biodegradable Nanomedicine for Cancer-Selective Dual-Modal Imaging Guided Precise Photodynamic Therapy, *Biomaterials*, 2019, **207**, 39–48.

74 W. Zhai, Y. Zhang, M. Liu, H. Zhang, J. Zhang and C. Li, Universal Scaffold for an Activatable Photosensitizer with Completely Inhibited Photosensitivity, *Angew. Chem., Int. Ed.*, 2019, **58**, 16601–16609.

75 A. P. Castano, T. N. Demidova and M. R. Hamblin, Mechanisms in Photodynamic Therapy: Part Three—Photosensitizer Pharmacokinetics, Biodistribution, Tumor Localization and Modes of Tumor Destruction, *Photodiagn. Photodyn. Ther.*, 2005, **2**, 91–106.

76 Y. Li, T. Y. Lin, Y. Luo, Q. Liu, W. Xiao, W. Guo, D. Lac, H. Zhang, C. Feng, S. Wachsmann-Hogiu, J. H. Walton, S. R. Cherry, D. J. Rowland, D. Kukis, C. Pan and K. S. Lam, A Smart and Versatile Theranostic Nanomedicine Platform Based on Nanoporphyrin, *Nat. Commun.*, 2014, **5**, 4712.

77 C. Yuan, W. Ji, R. Xing, J. Li, E. Gazit and X. Yan, Hierarchically Oriented Organization in Supramolecular Peptide Crystals, *Nat. Rev. Chem.*, 2019, **3**, 567–588.

78 M. Abbas, Q. Zou, S. Li and X. Yan, Self-Assembled Peptide- and Protein-Based Nanomaterials for Antitumor Photodynamic and Photothermal Therapy, *Adv. Mater.*, 2017, **29**, 1605021.

79 K. Liu, R. Xing, Q. Zou, G. Ma, H. Mohwald and X. Yan, Simple Peptide-Tuned Self-Assembly of Photosensitizers towards Anticancer Photodynamic Therapy, *Angew. Chem., Int. Ed.*, 2016, **55**, 3036–3039.

80 M. H. Cho, Y. Li, P.-C. Lo, H. Lee and Y. Choi, Fucoidan-Based Theranostic Nanogel for Enhancing Imaging and Photodynamic Therapy of Cancer, *Nano-Micro Lett.*, 2020, **12**, 47.

81 D. Hu, L. Zhong, M. Wang, H. Li, Y. Qu, Q. Liu, R. Han, L. Yuan, K. Shi, J. Peng and Z. Qian, Perfluorocarbon-Loaded and Redox-Activatable Photosensitizing Agent with Oxygen Supply for Enhancement of Fluorescence/Photoacoustic Imaging Guided Tumor Photodynamic Therapy, *Adv. Funct. Mater.*, 2019, **29**, 1806199.

82 K. C. Lowe, Perfluorinated Blood Substitutes and Artificial Oxygen Carriers, *Blood Rev.*, 1999, **13**, 171–184.

83 L. H. Young, C. C. Jaffe, J. H. Revkin, P. H. McNulty and M. Cleman, Metabolic and Functional Effects of Perfluorocarbon Distal Perfusion During Coronary Angioplasty, *Am. J. Cardiol.*, 1990, **65**, 986–990.

84 C. I. Castro and J. C. Briceno, Perfluorocarbon-Based Oxygen Carriers: Review of Products and Trials, *Artif. Organs*, 2010, **34**, 622–634.

85 R. Li, K. Zheng, P. Hu, Z. Chen, S. Zhou, J. Chen, C. Yuan, S. Chen, W. Zheng, E. Ma, F. Zhang, J. Xue, X. Chen and M. Huang, A Novel Tumor Targeting Drug Carrier for Optical Imaging and Therapy, *Theranostics*, 2014, **4**, 642–659.

86 H. N. Xu, H. J. Chen, B. Y. Zheng, Y. Q. Zheng, M. R. Ke and J. D. Huang, Preparation and Sonodynamic Activities of Water-Soluble Tetra-alpha-(3-carboxyphenoxyl) Zinc(II) Phthalocyanine and Its Bovine Serum Albumin Conjugate, *Ultrason. Sonochem.*, 2015, **22**, 125–131.

87 X. Li, C. Y. Kim, S. Lee, D. Lee, H. M. Chung, G. Kim, S. H. Heo, C. Kim, K. S. Hong and J. Yoon, Nanostructured Phthalocyanine Assemblies with Protein-Driven Switchable Photoactivities for Biophotonic Imaging and Therapy, *J. Am. Chem. Soc.*, 2017, **139**, 10880–10886.

88 X. Li, B. Y. Zheng, M. R. Ke, Y. Zhang, J. D. Huang and J. Yoon, A Tumor-pH-Responsive Supramolecular Photosensitizer for Activatable Photodynamic Therapy with Minimal *In Vivo* Skin Phototoxicity, *Theranostics*, 2017, **7**, 2746–2756.

89 X. Li, C. Y. Kim, J. M. Shin, D. Lee, G. Kim, H. M. Chung, K. S. Hong and J. Yoon, Mesenchymal Stem Cell-Driven Activatable Photosensitizers for Precision Photodynamic Oncotherapy, *Biomaterials*, 2018, **187**, 18–26.

90 H. B. Cheng, X. Li, N. Kwon, Y. Fang, G. Baek and J. Yoon, Photoswitchable Phthalocyanine-Assembled Nanoparticles for Controlled ''Double-Lock'' Photodynamic Therapy, *Chem. Commun.*, 2019, **55**, 12316–12319.

91 X. Li, H. Fan, T. Guo, H. Bai, N. Kwon, K. H. Kim, S. Yu, Y. Cho, H. Kim, K. T. Nam, J. Yoon, X. B. Zhang and W. Tan, Sequential Protein-Responsive Nanophotosensitizer Complex for Enhancing Tumor-Specific Therapy, *ACS Nano*, 2019, **13**, 6702–6710.

92 X. Li, S. Yu, Y. Lee, T. Guo, N. Kwon, D. Lee, S. C. Yeom, Y. Cho, G. Kim, J. D. Huang, S. Choi, K. T. Nam and J. Yoon, *In Vivo* Albumin Traps Photosensitizer Monomers from Self-Assembled Phthalocyanine Nanovesicles: A Facile and Switchable Theranostic Approach, *J. Am. Chem. Soc.*, 2019, **141**, 1366–1372.

93 B. Sun, R. Chang, S. Cao, C. Yuan, L. Zhao, H. Yang, J. Li, X. Yan and J. C. M. van Hest, Acid-Activatable Transmorphic Peptide-Based Nanomaterials for Photodynamic Therapy, *Angew. Chem., Int. Ed.*, 2020, **59**, 20582–20588.

94 J. Gao, J. Li, W. C. Geng, F. Y. Chen, X. Duan, Z. Zheng, D. Ding and D. S. Guo, Biomarker Displacement Activation: A General Host-Guest Strategy for Targeted Phototheranostics *in vivo*, *J. Am. Chem. Soc.*, 2018, **140**, 4945–4953.

95 L. Wu, Y. Sun, K. Sugimoto, Z. Luo, Y. Ishigaki, K. Pu, T. Suzuki, H. Y. Chen and D. Ye, Engineering of Electrochromic Materials as Activatable Probes for Molecular Imaging and Photodynamic Therapy, *J. Am. Chem. Soc.*, 2018, **140**, 16340–16352.

96 T. Qi, B. Chen, Z. Wang, H. Du, D. Liu, Q. Yin, B. Liu, Q. Zhang and Y. Wang, A pH-Activatable Nanoparticle for Dual-Stage Precisely Mitochondria-Targeted Photodynamic Anticancer Therapy, *Biomaterials*, 2019, **213**, 119219.

97 P. C. Lo, Y. Li, P. Sun, L. Zhao, X. Yan and D. K. Ng, Ferric Ion Driven Assembly of Catalase-Like Supramolecular Photosensitizing Nanozymes for Combating Hypoxic Tumor, *Angew. Chem., Int. Ed.*, 2020, **59**, 23228–23238.

98 Y. Song, Y. Li, Y. Zhang, L. Wang and Z. Xie, Self-Quenching Synthesis of Coordination Polymer Pre-Drug Nanoparticles for Selective Photodynamic Therapy, *J. Mater. Chem. B*, 2019, **7**, 7776–7782.

99 S. Li, Q. Zou, Y. Li, C. Yuan, R. Xing and X. Yan, Smart Peptide-Based Supramolecular Photodynamic Metallo-Nanodrugs Designed by Multicomponent Coordination Self-Assembly, *J. Am. Chem. Soc.*, 2018, **140**, 10794–10802.

100 H. Zhang, K. Liu, S. Li, X. Xin, S. Yuan, G. Ma and X. Yan, Self-Assembled Minimalist Multifunctional Theranostic Nanoplatform for Magnetic Resonance Imaging-Guided Tumor Photodynamic Therapy, *ACS Nano*, 2018, **12**, 8266–8276.

101 X. Meng, J. Deng, F. Liu, T. Guo, M. Liu, P. Dai, A. Fan, Z. Wang and Y. Zhao, Triggered All-Active Metal Organic Framework: Ferroptosis Machinery Contributes to the Apoptotic Photodynamic Antitumor Therapy, *Nano Lett.*, 2019, **19**, 7866–7876.

102 F. Hu, D. Mao, Kenry, Y. Wang, W. Wu, D. Zhao, D. Kong and B. Liu, Metal–Organic Framework as a Simple and General Inert Nanocarrier for Photosensitizers to Implement Activatable Photodynamic Therapy, *Adv. Funct. Mater.*, 2018, **28**, 1707519.

103 X. Ma and Y. Zhao, Biomedical Applications of Supramolecular Systems Based on Host-Guest Interactions, *Chem. Rev.*, 2015, **115**, 7794–7839.

104 T. Volk, H. P. Fortmeyer, K.-H. Glisenkamp and M. F. Rajewsky, pH in Human Tumour Xenografts: Effect of Intravenous Administration of Glucose, *Br. J. Cancer*, 1993, **68**, 492–500.

105 J. Kneipp, H. Kneipp, B. Wittig and K. Kneipp, Following the Dynamics of pH in Endosomes of Live Cells with SERS Nanosensors, *J. Phys. Chem. C*, 2010, **114**, 7421–7426.

This journal is © The Royal Society of Chemistry and the Chinese Chemical Society 2021

Mater. Chem. Front., 2021, **5**, 1683–1693 | **1693**